

Oscillatory models of the hippocampus: A study of spatio-temporal patterns of neural activity

Roman Borisyuk^{1,2}, Frank Hoppensteadt³

¹ Centre for Neural and Adaptive Systems, School of Computing, University of Plymouth, Drake Circus, Plymouth, PL4 8AA, UK

² Institute for Mathematical Problems in Biology, Russian Academy of Sciences, Pushchiko, Moscow Region, 142 292, Russia

³ Center for Systems Science, Arizona State University, Tempe, AZ 85287-7606, USA

Received: 31 July 1998 / Accepted in revised form: 20 April 1999

Abstract. Spatial patterns of theta-rhythm activity in oscillatory models of the hippocampus are studied here using canonical models for both Hodgkin's class-1 and class-2 excitable neuronal systems. Dynamics of these models are studied in both the frequency domain, to determine phase-locking patterns, and in the time domain, to determine the amplitude responses resulting from phase-locking patterns. Computer simulations presented here demonstrate that phase deviations (timings) between inputs from the medial septum and the entorhinal cortex can create spatial patterns of theta-rhythm phase-locking. In this way, we show that the timing of inputs (not only their frequencies alone) can encode specific patterns of theta-rhythm activity. This study suggests new experiments to determine temporal and spatial synchronization.

1 Introduction

The hippocampus has been implicated in several prominent aspects of information processing, such as the formation of a space map for navigation (O'Keefe and Nadel 1978; Wilson and McNaughton 1993), short- and long-term memory (Zola-Morgan et al. 1986; Eichenbaum 1997), complex stimulus conditioning (Sutherland and Rudy 1989), focusing attention (Kryukov et al. 1990), and detecting new and significant stimuli and registering them in memory (Vinogradova 1995).

Detailed analysis of experimental data of cortico-hippocampal interplay is available (McNaughton et al. 1989; Miller 1991; Palm 1993; Bibbig et al. 1994; Dutar et al. 1995), and recent experimental results suggest that spatio-temporal coherence of activity in the hippocampus (such as theta and gamma rhythms and sharp waves) could provide basic mechanisms for the wide spectrum of functional capabilities observed in hippocampus (Buzsaki 1994; Gray 1994; Vinogradova 1995; McNaughton et al. 1996; Tsukada et al. 1996).

There has been increasing interest in recent years in modeling the dynamics of hippocampal and cortical activity in order to gain insight into their functions (Traub and Miles 1991; Berger et al. 1994; Burgess et al. 1994; Treves and Rolls 1994; Blum and Abbot 1995; Hasselmo et al. 1995; Tsodyks and Sejnowski 1995; Traub et al. 1997; Ventriglia 1998).

In order to investigate the functional role of coherent activity in the brain, oscillatory neural network (ONN) models of various neural structures have been developed (Borisjuk et al. 1992; Hoppensteadt 1997). In ONNs, single neurons or populations of neurons have oscillatory activities that might be highly irregular, and process information using both frequency and the timing of signals. Analysis of these models is carried out here in both the time and frequency domains.

In this paper, we study the dynamics of oscillatory neural network models of the hippocampus by considering two elementary canonical models that describe systems that are of Hodgkin's class-1 and class-2 excitability (Hodgkin 1948; Hoppensteadt and Izhikevich 1997). These models take into account some important features of the three-dimensional structure of the hippocampus that are known from experiments. Each model is designed as a chain of interactive oscillators with natural frequency in the gamma range (40 Hz). Two primary external periodic inputs are considered: one from the entorhinal cortex and one from the medial septum. Both inputs are engaged in slow theta-rhythm oscillations (5 Hz), but there are some phase differences between them. It is shown here that such phase deviations can control spatial and temporal patterns of hippocampal activity. We demonstrate this interesting phenomenon using both frequency and time domain methods.

Our approach to modelling the hippocampus is described in Sect. 2. In Sect. 3, the frequency domain model is analyzed using mathematical analysis and computer simulations, and we determine explicitly the dependence of firing frequency patterns on the phase deviations between the two inputs. This suggests that spatial patterns of phase locking can encode phase deviations between the inputs. In Sect. 4, we investigate the amplitude dynamics of time domain models using

computer simulations. Our results using these two approaches to modeling are consistent. These and other conclusions are discussed in Sect. 5.

2 Oscillatory model of the hippocampus: global description

Physiological and anatomical experiments revealed the complex three-dimensional structure of the hippocampus (Isaacson 1982; Amaral and Witter 1989). One can visualize the hippocampus as being a three-dimensional structure having a long septotemporal axis and two transverse axes that are orthogonal to the long axis. Each two-dimensional slice perpendicular to the longitudinal axis contains three main regions called the dentate gyrus (DG), the CA₁ field, and the CA₃ field. These regions include both excitatory pyramidal neurons and inhibitory interneurons. The connections between hippocampal neurons are as extensive and highly organized in the septotemporal axis of the hippocampus as in the transverse axes (Amaral and Witter 1989). The neural populations located in each region can support endogenous oscillatory behavior without any external periodic input. There is some experimental evidence that the natural frequency of the endogenous oscillations are in the range of gamma rhythms (40–70 Hz) (Traub and Miles 1991; Buzsaki et al. 1994).

As a first step in developing our model, we neglect the fine structure of a two-dimensional slice that is transverse to the long axis. Instead, we model the interactive excitatory and inhibitory neural populations in the thin slice as being an oscillator, and we model the hippocampus as being a chain of such oscillators, S_1, S_2, \dots, S_N . We suppose that a single oscillator working independently demonstrates high frequency regular oscillations in the gamma range. Inputs to and coupling between these oscillators are discussed later. The lumping of complicated slices is a mathematical procedure used for studying spatially distributed structures. There is no morphological evidence of slice or segment structures in the hippocampus.

Two primary inputs to the hippocampus are considered here. These are currents injected along the septotemporal axis. Specifically:

1. I_C denotes an input from afferents of the entorhinal cortex;
2. I_S denotes an input from the medial septum.

Morphological and physiological data suggest that both of these inputs distribute information among the hippocampal oscillators and that they oscillate at (nearly) identical frequencies. Both inputs are low frequency (3–9 Hz) theta rhythms (Vinogradova 1995; Iijima et al. 1996).

Experimental evidence by Amaral and Witter (1995) shows that the septal end of the entorhinal cortex projections to the hippocampus are topographically organized. Cells located medially in the medial septum tend to project to the septal part of the hippocampus and cells located laterally tend to project to the hippocampal

temporal regions. The entorhinal cortex projections demonstrate similar organization: cells located laterally in the entorhinal cortex project to more septal regions of the hippocampal fields, whereas cells located progressively more medially project to more temporal parts of the hippocampus. Our model development is based on the hypothesis that the spatial distribution of inputs causes appropriate time delays, which result in phase lags. The activity of a hippocampal oscillator depends on interactions between the theta-rhythm modulated cortical input I_C and the oscillatory signal I_S from the medial septum. The models studied here are shown to depend on the deviation in timing between these two low frequency inputs. We show here that the frequencies of the input signals and their phase relations determine which segments of the hippocampus model exhibit synchronous low frequency activity and which do not.

The influence of these low frequency oscillatory inputs results in complex dynamics, including entrainment, chaotic behavior, and envelop oscillations.

Two principal outputs from the hippocampus are as follow:

1. The CA₃ output is carried by axon collaterals of pyramidal cells of the CA₃ field. This output completes a feedback loop from the hippocampus to the lateral septum, which can reset the timing of the medial septum. By means of this loop, the activity level of pyramidal cells of the CA₃ field can control the theta-rhythm generated in the medial septum.
2. The CA₁ output is carried by axon collaterals of pyramidal cells of the CA₁ field. This output completes a feedback loop (reverberating activity loop) to the cortex through the subiculum.

These feedback circuits are not discussed further here.

As the external signals are distributed along the hippocampus, phase deviations arise between them. These specific time delays are taken into account by assuming that for each oscillator, say S_n ($n = 1, 2, \dots, N$), the time delay of the cortical input I_C to the slice oscillator is $(n - 1)\Delta t$ and the time delay for the septal input I_S is $(N - n)\Delta t$, where Δt is the propagation time between two oscillators for I_C and I_S . Experiments (O'Keefe and Nadel 1978; Buzsaki et al. 1994; Bragin et al. 1996) indicate that theta-rhythm activity propagates along the hippocampus during τ ms (τ is in the range 25–50 ms) so the value of Δt is taken to be t/N ms, etc. The result is that the net input to an oscillator involves a signal having a theta-rhythm frequency and a phase deviation that is related to its location along the hippocampus.

From a mathematical point of view, the model of the hippocampus is considered as being a system of interacting oscillators. A single oscillator working independently shows fast regular oscillations with high frequency in the gamma range (40 Hz), and each oscillator has two slow oscillatory inputs with frequencies in the theta range (5 Hz) but (usually) of different phases. Due to the time delays in the input signals, two traveling waves arise and propagate along afferents as inputs to the hippocampus, but in contrary directions. The interference patterns created by these waves make possible

the appearance of synchronization, coincidence and non-linear resonance patterns. This means that the activity level of some hippocampal oscillators increases due to specific relations between frequencies of inputs and phase deviations between them. In this sense, the hippocampal model works like a spatial ‘comparator’ that compares two input signals at an oscillator and, in turn, reacts or not (cf. ‘‘phase precession’’ effect by O’Keefe and Recce 1993 and Skaggs 1995; Fig. 1).

General systems theory provides some guides for modeling such networks of coupled oscillators (Borisjuk et al. 1995; Hoppensteadt and Izhikevich 1997). This is based on the bifurcation theory that concentrates on how a system behaves near critical regimes. For example, a system’s behavior can change from rest to oscillation, and this is described mathematically by a hierarchy of mathematical models, called bifurcation equations, that have increasing complexity. The complexity of each is described by how many (dimensionless) parameters are needed for it. This number is called the co-dimension of the bifurcation. For example, there are two co-dimension one bifurcations that give rise to oscillations. One exhibits the onset of oscillation as being of fixed amplitude and with frequencies increasing from zero as the bifurcation parameter passes through the critical value. This is a saddle-node on limit cycle (SNLC) bifurcation. The second is a supercritical Andronov-Hopf bifurcation in which an oscillation of fixed frequency but increasing amplitude appears (Hoppensteadt and Izhikevich 1997). Another step in the hierarchy is the separatrix loop bifurcation, which has co-dimension two. It allows the coexistence of stable equilibrium and stable oscillations, and a hysteresis between them. The oscillators in this hierarchical list quickly become quite complicated. Oscillatory solutions are defined by their geometrical features, and they are described mathematically by equations called canonical models.

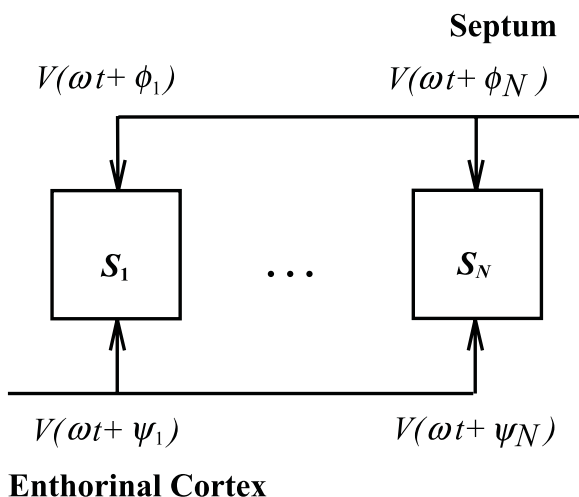


Fig. 1. An oscillatory model comprising N oscillators that have inputs from the septum and from the entorhinal cortex that are a fixed waveform (V) with fixed frequency (ω) and phase deviations (ϕ_j or ψ_j , respectively)

The usual approach to modeling complex systems is to begin with the simplest canonical model, derive results about it and compare the results with simulations and experiments. We do this here by first using mathematical analysis to derive pattern criteria, then we investigate patterns using computer simulations. We use the VCON model (Hoppensteadt 1997), also referred to here as the phase oscillator model. In this case, we are able to derive results about patterns of synchronization through rigorous analysis in the frequency domain. Second, we study a system of coupled neural oscillators of the Wilson-Cowan type. While these are not actually canonical models for Andronov-Hopf bifurcations, they share many properties with them and are widely understood, especially regarding how they can be networked. The amplitude responses of these systems are investigated using computer simulations.

3 Phase model

In this section, we study the dynamics of large-scale networks where each oscillator is described by only one variable, its current phase of oscillation. Using this approach, we are able to obtain theoretical estimates of phase-locking regimes and to perform simulations that exhibit such patterns.

Signals are described in terms of a variable phase, say θ , and a fixed waveform, say V [for example, $V(\theta) = \sin(\theta)$]. Since signals are usually oscillatory, we refer to θ as being the oscillation’s phase. This might represent the phase of the membrane potential in the hillock region of a single neuron or the phase of the average oscillatory activity of a large neural assembly. This variable is particularly useful for mathematical and computational analysis of interactions and synchronization between several neural assemblies (Hoppensteadt 1997). While it might seem to be oversimplified, this model is a canonical model describing the onset of oscillations through an SNLC bifurcation. Analysis of phase oscillators enables us to describe regions of parameter space associated with different types of dynamic behavior in the frequency domain, such as general or partial synchronization (Kazanovich and Borisjuk 1994; Borisjuk and Kazanovich 1995).

In many cases, the phase settles down to the form $\theta = \omega t + \varphi$ where t is time measured in some convenient units, ω is frequency and φ is the phase deviation satisfying $\varphi/t \rightarrow 0$ as $t \rightarrow \infty$. Signal processing methods can be used to determine the frequency ω and the phase deviation φ in the presence of noise and under constantly changing conditions. Such methods are based on analysis in the frequency domain.

Phase models result from canonical model analysis of real networks that involve a system near an SNLC or a separatrix-loop bifurcation (Hoppensteadt and Izhikevich 1997). They are canonical in the sense that any network having an SNLC bifurcation can be reduced near it to this model, and all of the other variables are subsidiary and can be ignored. In this sense, canonical models are independent of the general system being considered, and

they can be described in terms of behavior of solutions rather than in detailed mathematical formulations.

3.1 Mathematical analysis

We describe the dynamics of a hippocampal oscillator, say S_n , using a VCON model (Hoppensteadt 1997). We omit the oscillator index n below to simplify formulas:

$$d\theta/dt = \gamma + \cos \theta + K[\cos \theta_C(t) + \cos \theta_S(t)](1 - \cos \theta) \quad (1)$$

where γ is a natural frequency of the phase oscillator ($\gamma \approx 2\pi \cdot 40$), K is the gain of the input, and we suppose that the phases of the cortical and septal inputs, respectively, are

$$\theta_C = \omega_0 t + \phi_C, \quad \theta_S = \omega_0 t + \phi_S \quad (2)$$

where ω_0 is the theta-rhythm frequency ($\omega_0 \approx 5$ Hz).

We use as an approximation to this model one obtained by formally averaging it over t . Substituting $\bar{\phi} = (\phi_C + \phi_S)/2$ and $\Phi = \theta - \omega_0 t - \bar{\phi}$ results in an equation for studying phase locking

$$d\Phi/dt = \gamma - \omega_0 - K \cos \Phi \cos \psi \quad (3)$$

where $\psi = (\phi_C - \phi_S)/2$ is the phase deviation between the two inputs from the cortex and the septum, respectively. This equation will have a stable rest point, say Φ^* , if the condition for phase locking,

$$\left| \frac{\gamma - \omega_0}{K \cos \psi} \right| \leq 1 \quad (3)$$

is satisfied, in which case

$$\Phi^* = \arccos \frac{\gamma - \omega_0}{K \cos \psi} \quad (3)$$

The condition for phase locking depends on three parameters: K , $\Omega = \gamma - \omega_0$, ψ . The regions of phase-locking with the theta rhythm in the (ψ, Ω) plane for several values of the parameter K are shown in Fig. 2. These simple graphs demonstrate that, for fixed oscillator natural frequencies, there are two intervals of phase deviation values for which phase locking occurs. The region of phase locking with the theta rhythm increases with increasing values of the parameter K .

3.2 Computer simulations of VCON model

In this section, we consider the full VCON model of a slice oscillator having lateral connections that are local and weak.

$$d\theta_n/dt = \gamma + \cos 2\pi\theta_n + K \left[\cos \theta_C + \cos \theta_S + \varepsilon \sum_{j=-3, j \neq 0}^3 C_j \cos 2\pi\theta_{n+j} \right] \times (1 - \cos 2\pi\theta_n) \quad (4)$$

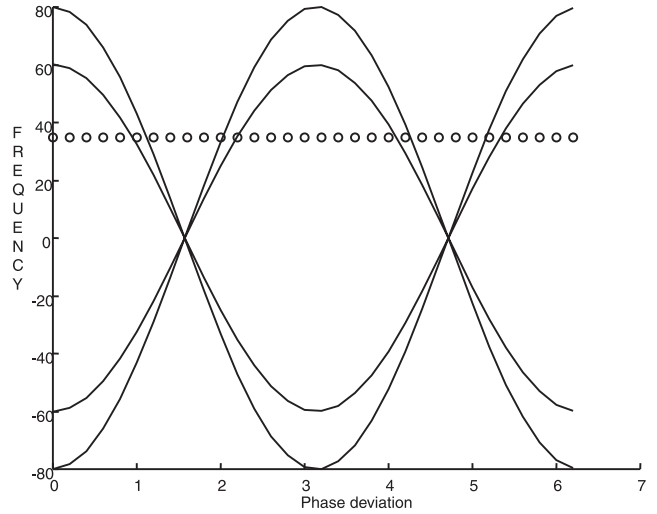


Fig. 2. The boundary of predicted phase locking as contours of Ω and ψ for various values of K ($K = 80$, $K = 60$). Horizontal line of o 's corresponds to frequency values $\gamma = 40$, $\omega_0 = 5$. The region inside boundaries relates to phase locking with a theta rhythm

where $n = 1, 2, \dots, N$, θ_n is the phase of n th oscillator, γ is a natural frequency of the VCON oscillator ($\gamma \approx 40$ Hz), K is the strength of the input's influence, and we suppose that influences of the cortical (θ_C) and septal (θ_S) inputs are given by Eq. (2); ε is a small parameter that describes the weak influence of the nearest oscillators (if they exist). The study of Eq. (4) exhibits the same phenomenon as the simplified phase-oscillator model (1); namely, the spatiotemporal pattern of neural activity depends critically on ψ , which measures the phase deviation between two inputs.

We corroborated this phenomenon with computer simulations of the VCON model using the phase-locking condition (3) as a guide for the selection of parameters. The results of these simulations are shown in Figs. 3 and 4. They demonstrate the parts of the oscillatory neural network, for the parameters indicated in the figure caption, that do phase lock to a theta rhythm for some phase deviations ψ , and that they oscillate near the gamma rhythm for others. The phase-locking pattern is shown in

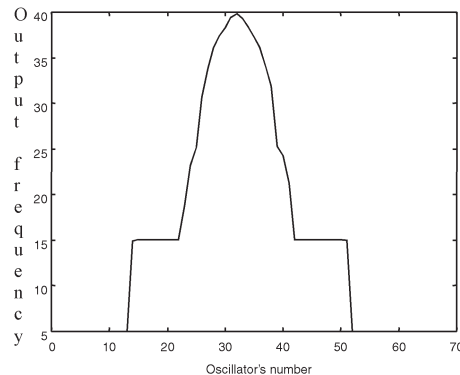


Fig. 3. Frequency output of oscillators as a function of input phase deviations. The vertical axis gives the output frequency and the horizontal axis gives the location. Here, $N = 64$

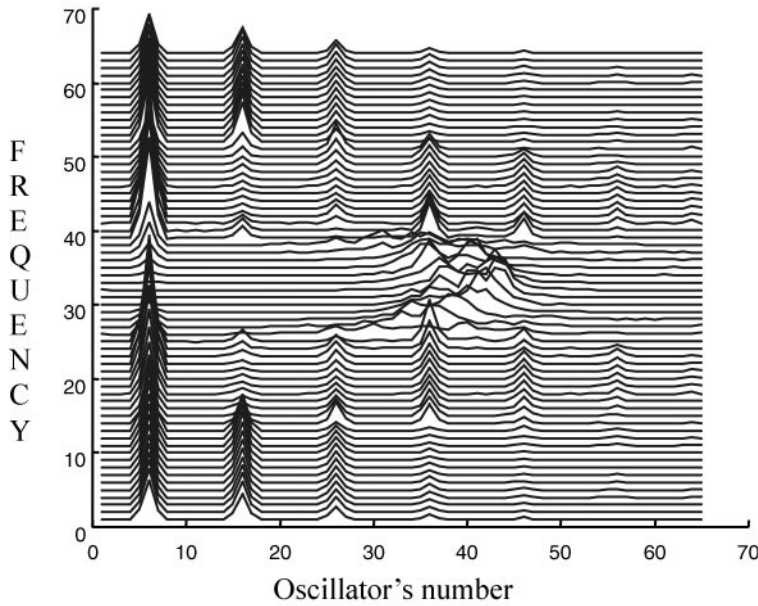


Fig. 4. Power spectrum of each oscillator simulated in Fig. 3. Here, each line on starting at the *vertical axis* gives the power spectrum of the oscillator at that location. The *horizontal axis* gives the frequency

Fig. 3, where the output frequency of each oscillator, $\bar{\Omega} = \lim_{t \rightarrow \infty} \theta(t)/t$, is plotted. The power spectrum of the oscillators is shown in Fig. 4, which shows that the output frequencies are quite rich for most deviations ψ .

If we consider a VCON oscillator forced by signals having nearly the same phase, and if the phase deviations are chosen near zero or near π , then those oscillators have similar steady-state phase deviations and the model of the hippocampus will demonstrate almost synchronous oscillations throughout. This result agrees with experimental evidence showing synchronous oscillation of the whole hippocampus with the theta rhythm (B. McNaughton, personal communication). Another choice of phase deviation of inputs gives another pattern of oscillations. For example, for a phase deviation near $\pi/2$, some oscillators will be out of lock. The power spectrum of each of the 64 oscillators is shown in Fig. 4.

This analysis of the phase oscillator model and computer simulations of the VCON model show that the timing of inputs to an oscillator can result in a dramatic change in its firing frequency. In particular, various timing combinations can create characteristic patterns of theta-rhythm activity in the array of oscillators.

4 Amplitude model

In this section, we consider each oscillator S_n to be described by a set of two interacting neural populations: excitatory and inhibitory. We refer to this model as being the amplitude model or neural oscillator (Wilson and Cowan 1972). This model enables us to study the dynamics of average neural activity (roughly analogous to the EEG signal) under a variety of connection schemes.

The amplitude model is described by the equations

$$\begin{cases} dE_n/dt = -E_n + (k_e - E_n)Z_e(c_1E_n - c_2I_n + P_n + R_n), \\ dI_n/dt = -I_n + (k_i - I_n)Z_i(c_3E_n - c_4I_n + Q_n + V_n), \\ n = 1, \dots, N. \end{cases} \quad (5)$$

Here, $E_n(t), I_n(t)$, are the activities of excitatory and inhibitory populations of the oscillator number n ; c_1, c_2, c_3, c_4 are positive parameters showing the coupling strengths between different types of populations ($c_1 = 16, c_2 = 12, c_3 = 15, c_4 = 3$); P_n and Q_n are the values of the external inputs to the excitatory and inhibitory populations, respectively; $Z_p(x) = Z_p(x; b_p, \theta_p)$ are monotonically increasing sigmoid-type functions,

$$Z_p(x) = 1/\{1 + \exp[-b_p(x - \theta_p)]\} - 1/[1 + \exp(b_p\theta_p)], \quad p \in \{e, i\},$$

where $b_e, \theta_e, b_i, \theta_i$ are constants ($\theta_e = 4, b_e = 1.3, \theta_i = 2, b_i = 2$); $N = 64$; k_p is a constant and $k_p = 1/Z_p(+\infty)$. R_n and V_n account for interoscillator connections. It was shown in Borisyuk et al. (1995) that the dynamics of neural activity depends sensitively on the type of connections (excitatory-excitatory, inhibitory-inhibitory, from excitatory to inhibitory, and from inhibitory to excitatory) and each connection type is characterized by a specific spatiotemporal pattern. We consider here the connection architectures of various types, including local, global and random connections between oscillators. In all cases that we have considered, the same phenomena occur; the spatiotemporal pattern of neural activity is sensitive to the phase deviation between the two inputs.

We suppose that the input from the entorhinal cortex has influence only on the excitatory population and that the input from the septum only has influence on the inhibitory population. The external input to the model has the form

$$\begin{aligned}
P_n &= \bar{P} + \beta_C \cos \left[\frac{2\pi}{T} (t + \phi_C) \right], \\
Q_n &= \beta_S \left\{ 1 + 3 \cos \left[\frac{2\pi}{T} (t + \phi_S) \right] \right\},
\end{aligned} \tag{6}$$

where \bar{P} describes the total non-specific influence to the excitatory population; β_C describes the strength of a specific sensory input from the entorhinal cortex to the excitatory neurons; T is the period of theta-rhythm oscillations; ϕ_C is a phase shift of the cortical input; β_S measures the strength of influence of the septal input; ϕ_S is the phase shift of the septal input.

Experimental evidence does not yet tell us how to select parameters in these models. It is known that populations of interactive excitatory and inhibitory neurons are able to exhibit oscillatory behavior. Some experimental evidence (e.g., recordings on hippocampal slices) shows that if the endogenous oscillations of a single hippocampal oscillator are possible, then the period of oscillations is 20–50 ms (i.e., 20–50 Hz) (Buzsaki et al. 1994; Traub et al. 1996).

The parameter \bar{P} controls the oscillatory activity of a single oscillator. If the value of this parameter is small, then only steady states with low activity levels exist. If the parameter \bar{P} increases, the limit cycle appears through a separatrix loop bifurcation ($\bar{P} = 1.17$) and it disappears through an Andronov-Hopf bifurcation ($\bar{P} = 1.8$) (Borisjuk and Kirillov 1992). For a wide range of parameter \bar{P} values ($1.4 < \bar{P} < 1.7$), the limit cycle exists and its period varies from large to small values (with average period value about 4).

We will consider both the case of steady-state behavior of a single oscillator ($\bar{P} = 1$) and the case of endogenous oscillations of a single oscillator. In the case of oscillations, we choose the value of parameter $\bar{P} = 1.5$, and an oscillation period is about 4 units of the model's time. We suppose that this period (4 units of model time) corresponds to 20 ms oscillation period in experimental recordings. This correspondence makes it possible to establish a time scale: one unit of the model's time is proportional to 5 ms. Hence, the period of the theta rhythm (200 ms) corresponds to 40 time units of model time [$T = 40$ in Eq. (6)].

Note that the septal input I_S inhibits the activity of inhibitory neurons. It switches off their influence for some time less than the half-period of the theta rhythm, and it allows pyramidal cells (the excitatory population) to increase their activity. Thus, it is possible for there to be a theta rhythm in a hippocampal oscillator. The influence of the second input (from the entorhinal cortex) to the excitatory neurons, which is also modulated by the theta-rhythm frequency, leads to a complex non-linear interaction of signals. The dynamics of the oscillator S_n results from this interaction.

4.1 Steady-state behavior of a single oscillator

In this section, we consider the case where each single oscillator demonstrates steady-state behavior. We

choose the value $\bar{P} = 1.0$ that corresponds to a low-level stationary background activity of a single oscillator. We study both the dynamics of a single oscillator and the dynamics of coupled oscillators with different connection types. Experimental evidence on intrahippocampal connections between pyramidal neurons (Ishizuka et al. 1990) shows complex organization of the connection, both along the septotemporal axis and transversally. We suppose that a thin hippocampal slice perpendicular to the septotemporal axis contains interconnected pyramidal neurons and interneurons, which form a neural oscillator. Connections between oscillators reflect a complex topology of intrahippocampal projections originating from pyramidal cells along septotemporal axis. Our models are very coarse and they do not take the fine details of the nature of these connections into account. Nevertheless, we consider different connection types to exist between oscillators (local, all-to-all, and random) and show that for each case a spatiotemporal pattern of neural activity mainly depends on phase deviations between the two inputs.

Note that generally oscillatory behavior of the model is possible due to both the interactions between oscillators and the external oscillatory inputs. For example, if both external inputs are not effective [in Eq. (6) $\beta_C = 0$ and $\beta_S = 0$], then oscillatory behavior occurs for all-to-all connections between excitatory populations with connection strengths randomly and uniformly distributed between 0 and 0.1 [see Eq. (7)]. The spatiotemporal pattern of these oscillations is shown in Fig. 5. The oscillations are regular and coherent with a period of about 4 time units (20 ms). This result demonstrates that a gamma rhythm might appear due to interactions between single slice oscillators with low-level stationary activities.

When only the septal input is effective ($\beta_C = 0$, $\beta_S \neq 0$), the period of hippocampal oscillators is about 200 ms and phase locking with a theta rhythm appears. When both inputs are effective, the amplitude of the oscillatory activity depends on the phase deviation between the input signals. Figure 6 shows the maximal amplitude of an oscillation from the excitatory population of a single oscillator plotted against the phase deviation. At some values of the phase deviation, the amplitude of the activity is quite large. This is similar to the predictions of the frequency domain analysis. For some values of the phase deviation, the amplitude is rather small, and the activity is out of phase-lock with the theta rhythm.

There is a critical value of the phase deviation where the amplitude of oscillations 'jumps' from small to large values. Figure 7 shows two limit cycles, the smaller one corresponds to $\psi = 26.6808$ and the larger one corresponds to $\psi = 26.6809$!

4.1.1 Local connections

We show here that, while single oscillators in this case are stationary with a low activity level ($\bar{P} = 1$), collective interactions of the entire set of slice oscillators and two external inputs can exhibit interesting spatiotemporal patterns of oscillations.

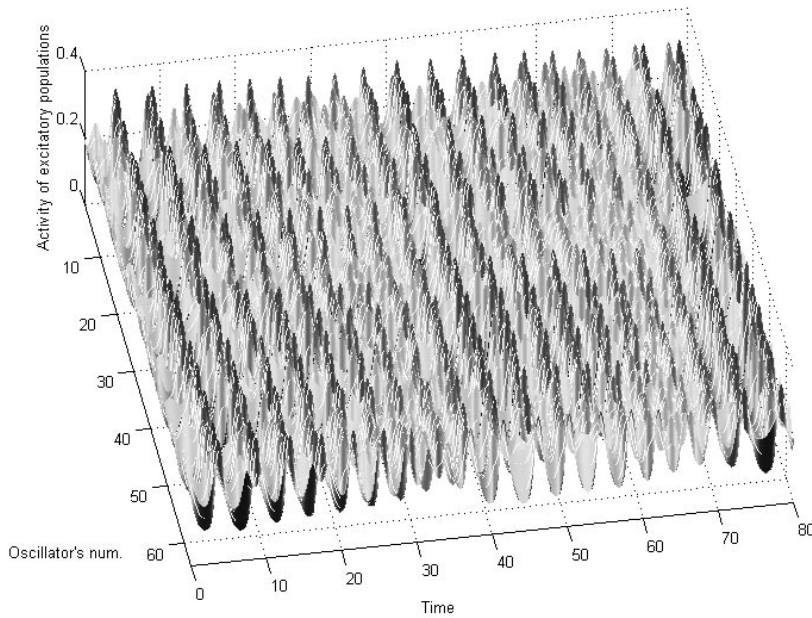


Fig. 5. An example of gamma oscillations arising due to interactions between single oscillators with low-level stationary activity. [$\beta_C = 0$, $\beta_S = 0$, $\bar{P} = 1$, $Q_n = 0$, R_n is given by Eq. (7), $W_n = 0$, $N = 64$]

Consider a chain of locally coupled oscillators forced by input signals I_C and I_S with appropriate phase delays as described above. While we can consider all four types of connections (excitatory-excitatory, inhibitory-inhibitory, from excitatory to inhibitory and from inhibitory to excitatory), we present results here for the first case. All other cases also exhibit dependence of the spatio-temporal pattern of neural activity on a phase deviation between oscillators.

Each oscillator receives six connections: three from the left and three from the right. The connection strength decreases with distance from the oscillator. For example, the influence of the nearest oscillators to the n th oscillator for the excitatory-excitatory symmetric connections is given by

$$R_n = \sum_{j=-3, j \neq 0}^3 \alpha_j E_{n+j}, \quad V_n = 0,$$

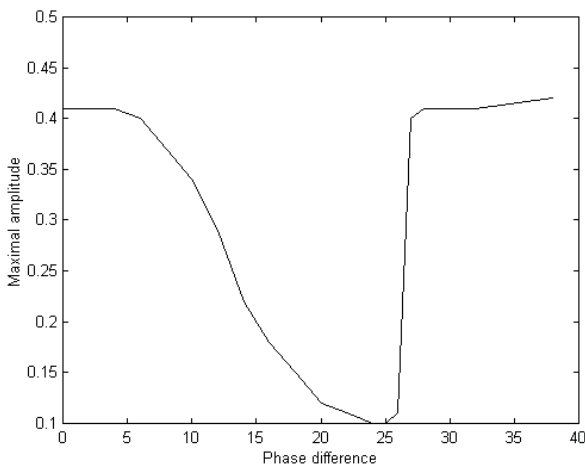


Fig. 6. The maximal amplitude of excitatory population activity for a single slice oscillator versus the phase deviation of input signals $\psi = \phi_C - \phi_S$. ($0 < \phi_C < 40$, $\phi_S = 0$, $\beta_C = 0.2$, $\beta_S = 1.5$, $T = 40$, $\bar{P} = 1$, $Q = 0$, $R = 0$, $W = 0$, $N = 1$).

where α_j decreases with the distance $|j|$. Here, we simply ignore the terms with indexes that are out of range.

The value of Δt , introduced in Sect. 2, is chosen in a such way that the traveling time of a signal along the whole hippocampus is about 50 ms (one fourth of the theta-rhythm period) (O'Keefe and Nadel 1978). Figure 8A,B shows the activities of the excitatory populations of different oscillators of the hippocampus with different values of phase deviation between inputs. At particular values of the phase deviation, some oscillators either have a low level of activity or are completely inactive (Fig. 8A). Nevertheless, there are values of the phase deviation that cause high activity levels in the pyramidal cells in all hippocampus oscillators (Fig. 8B).

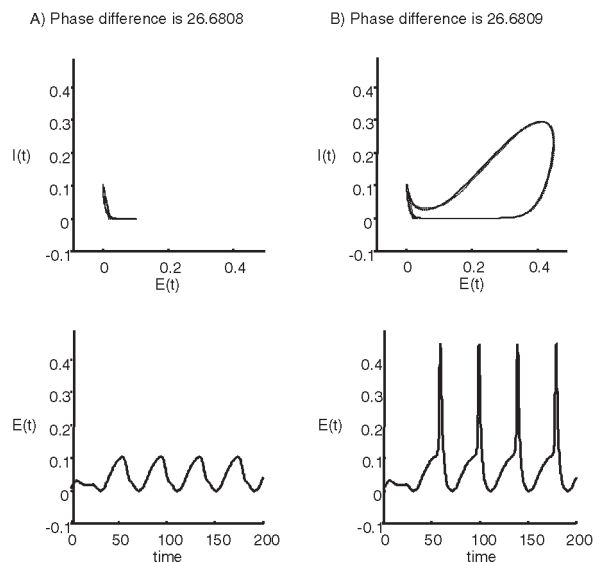


Fig. 7A,B. The limit cycle of a single slice oscillator for two very close values of a phase deviation (parameter values are the same as in caption to Fig. 6). **A** Phase deviation $\psi = 26.6808$; **B** phase deviation $\psi = 26.6809$

The results for the other connection types between oscillators are similar.

4.1.2 All-to-all connections

We suppose here that each oscillator has connections with all other hippocampal oscillators. The connection type is excitatory-excitatory and the connection values are randomly distributed as before. The connection terms in Eq. (5) are now

$$R_n = \sum_{j=1, j \neq n}^N w_{nj} E_j, \quad V_n = 0, \quad (7)$$

where w_{nj} are random variables that are uniformly distributed between 0 and 0.1. The resulting spatiotemporal pattern of oscillatory activity is shown in Fig. 9. Other connection types give rise to similar phase-deviation dependent spatiotemporal dynamics of neural activity (not shown).

4.1.3 Random connections

Here, we consider the chain of 64 oscillators each having 30 random connections. The excitatory population of each oscillator receives connections from 30 neural populations, excitatory or inhibitory. These populations are randomly chosen between 126 possible populations of other oscillators. The connection strengths also are randomly chosen, with their absolute values distributed uniformly between 0 and 0.5. The connection strengths are negative for terms including the influence of the inhibitory population and connection strengths are positive for the terms including the influence of an excitatory population.

Figure 10 shows two spatiotemporal patterns of neural activity corresponding to two different values of phase deviation ψ . Almost all oscillators shown in Fig. 10A ($\psi = 17$) exhibit large amplitude synchronous oscillations at the theta frequency. Another spatiotemporal pattern, corresponding to the phase deviation value $\psi = 37$, is shown in Fig. 10B. There is a large

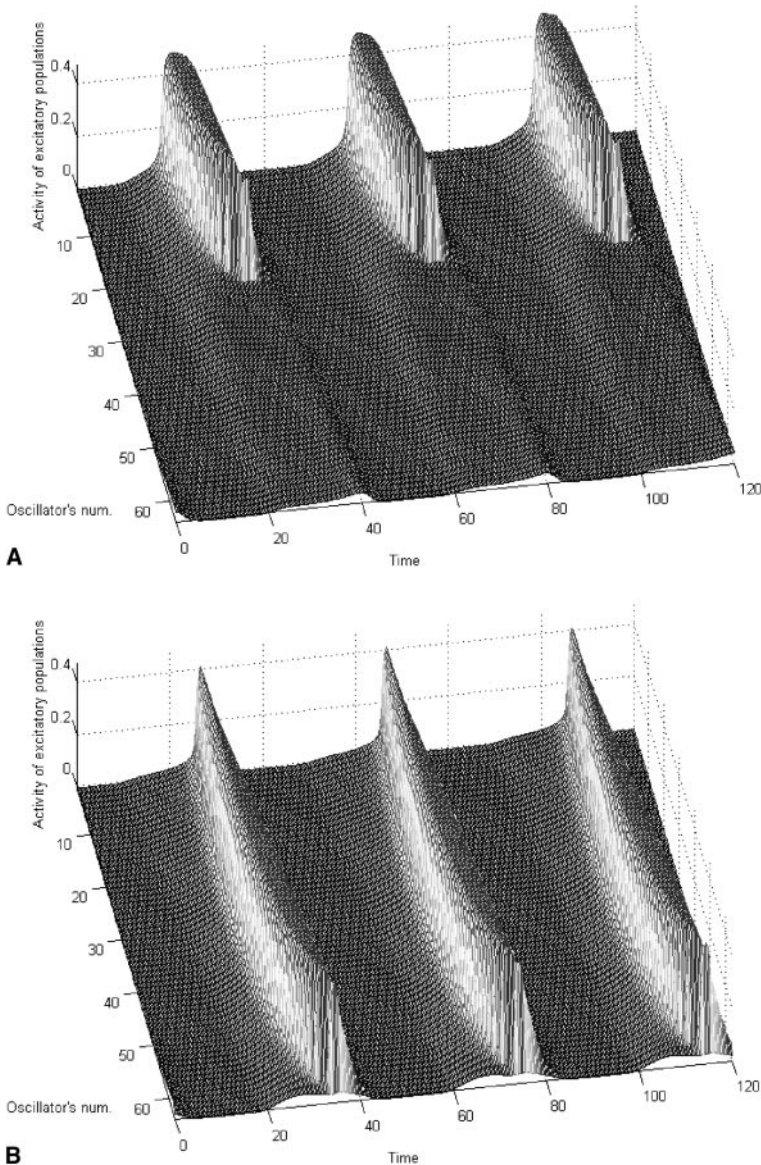


Fig. 8A,B. Local connections. The spatiotemporal patterns of activity for different values of phase deviation ψ ($0 < \psi < 40$), $\phi_S = 0$, $\beta_C = 0.2$, $\beta_S = 1.5$, $T = 40$, $\bar{P} = 1$, $Q = 0$, $N = 64$, $\alpha_1 = 0.5$, $\alpha_2 = 0.1$, $\alpha_3 = 0.05$, $\alpha_{-1} = 0.5$, $\alpha_{-2} = 0.1$, $\alpha_{-3} = 0.05$, **A** $\psi = 5$; **B** $\psi = 18$

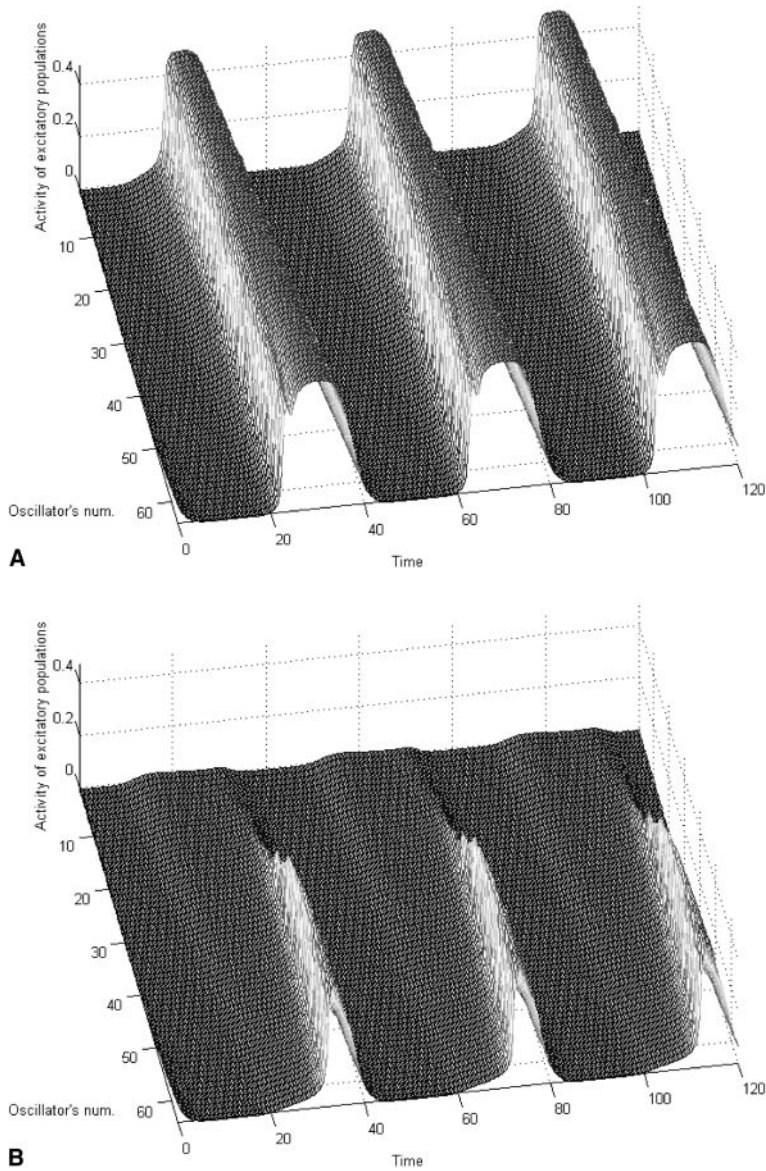


Fig. 9. All-to-all connections. The spatiotemporal patterns of activity for different values of phase deviation ψ ($0 < \psi < 40$), $\phi_S = 0$, $\beta_C = 0.2$, $\beta_S = 1.5$, $T = 40$, $\bar{P} = 1$, $Q = 0$, $N = 64$. The values of all-to-all excitatory connection strengths are uniformly distributed between 0 and 0.1, **A** $\psi = 5$; **B** $\psi = 35$

difference between oscillation amplitudes for different oscillators in this case.

4.2 Oscillatory behavior of a single oscillator

In this section, we consider the case of oscillatory activity of a single hippocampal oscillator. The value of the control parameter is $\bar{P} = 1.5$ and, the oscillation period is about 4 model time units (20 ms). We assume that the natural frequency of the oscillator is in the range of gamma oscillations (20–50 Hz). While we do not model the gamma oscillations, others have done so using fine synaptic processes and, in particular, GABA_A synaptic inhibition (Traub et al. 1996; Wang and Buzsa'ki 1996; Traub et al. 1997). In this case, a typical spatiotemporal activity pattern is a pattern of quasi-periodic (envelope) oscillations.

4.2.1 Envelope oscillations

Figure 11 shows the activity of the single hippocampal oscillator when both inputs to the oscillator are active. The envelope oscillations are rather typical for these values of parameters. The activity of excitatory neurons (pyramidal cells) in the model simulations is similar to the EEG activity in the range of the gamma rhythm recorded from the hippocampus (cf. Fig. 3B in Bragin et al. 1995). Figure 11B shows the activity of the single hippocampal oscillator in the case of a lesion eliminating the input from the entorhinal cortex ($\beta_C = 0$, $\beta_S \neq 0$). In this case, the 40-Hz oscillations almost completely disappear, and the 5-Hz oscillations dominate.

Figure 12 shows spatiotemporal patterns of activity for the case of random connections between oscillators. Each oscillator receives ten connections from neural populations (excitatory or inhibitory) of other oscillators. The values of connection strengths are randomly

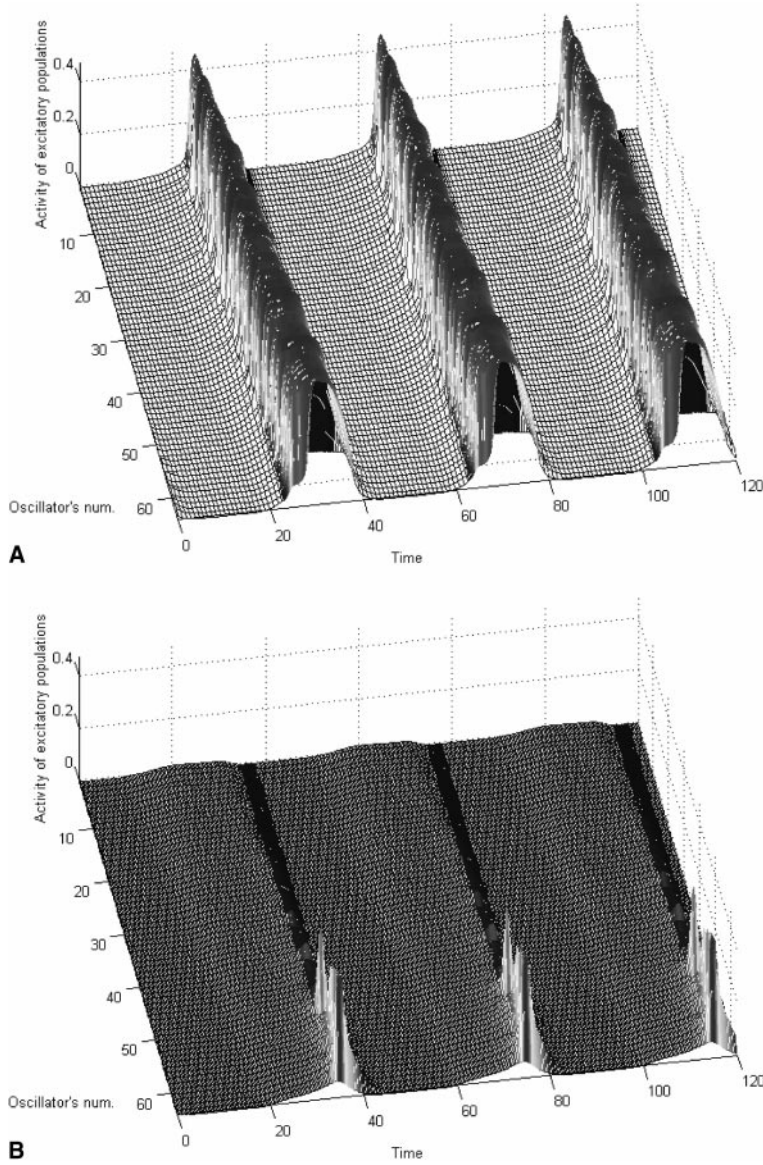


Fig. 10A,B. Random connections. The spatiotemporal patterns of activity for different values of phase deviation ψ ($0 < \psi < 40$), $\phi_S = 0$, $\beta_C = 0.2$, $\beta_S = 1.5$, $T = 40$, $\bar{P} = 1$, $Q = 0$, $N = 64$. The values of 30 randomly chosen connection strengths are uniformly distributed between 0 and 0.5. **A** $\psi = 17$; **B** $\psi = 37$

distributed between 0 and 0.1. Figure 12 shows the spatiotemporal activity where all oscillators are phase-locked with theta rhythm. Oscillations with a low index (location) have both gamma and theta rhythms and those at the other end have theta rhythms.

4.2.2 Lesion of the entorhinal cortex input

Our analysis suggests that if there is a lesion from the entorhinal cortex to the hippocampus and only input from the medial septum, then there is a uniform theta rhythm. Under these experimental conditions, the

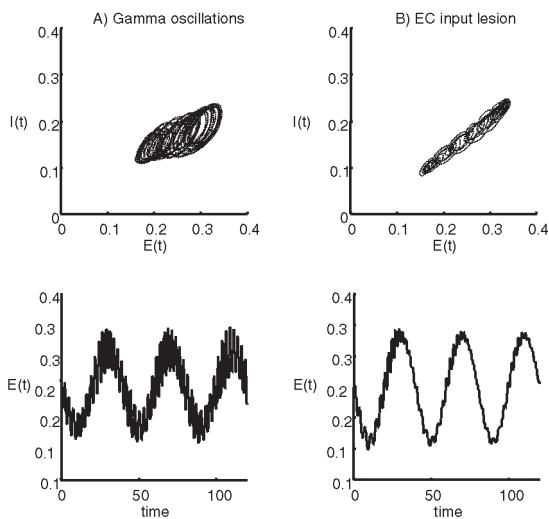


Fig. 11A,B. Phase portrait and dynamics of a single oscillator mode. **A** Envelope oscillations with both gamma and theta frequencies. ($\phi_C = 0$, $\phi_S = 20$, $\beta_C = 0.3$, $\beta_S = 0.25$, $T = 40$, $\bar{P} = 1.5$, $Q = 0$, $R = 0$, $W = 0$, $N = 1$). **B** Oscillations in the case of the entorhinal cortex lesion; the amplitude of gamma oscillations is very small ($\phi_C = 0$, $\phi_S = 20$, $\beta_C = 0$, $\beta_S = 0.25$, $T = 40$, $\bar{P} = 1.5$, $Q = 0$, $R = 0$, $W = 0$, $N = 1$)

amplitude of gamma rhythm is much smaller (only 20–30% of normal; Bragin et al. 1995). The result of computer simulations of the Eq. (4) is shown in Fig. 13. The spatiotemporal pattern corresponding to these experimental conditions demonstrates mostly theta rhythms and only oscillations with small amplitude are related to high frequency modes. In this simulation, we have used the same parameter values as in the simulation shown in Fig. 12, but with $\beta_C = 0$.

4.2.3 Lesion of the medial septum input

Lesion of the septal input has the opposite effect. Computer simulations of Eq. (4) are shown in Fig. 14. The spatiotemporal pattern corresponding to these experimental conditions demonstrates mostly gamma rhythms and only oscillations with a small amplitude are related to theta frequencies. In this simulation, we have used the same parameter values as in the simulation shown in Fig. 12, but with $\beta_S = 0$.

The simulations with lesions of different inputs show that both inputs are important for the creation of a spatiotemporal pattern of neural activity in the hippocampus, but the influence of each input has some specificity. The input from the entorhinal cortex provides mostly a high frequency part of multi-frequency oscillations and the input from the medial septum has a larger influence on a low frequency theta-rhythm region.

5 Discussion

The dynamics of a single hippocampal slice is modeled here first by a phase oscillator. We show that non-linear interactions between two periodic inputs result in phase-locking patterns that depend on the phase deviation between the input signals. In some range of phase deviations, the model demonstrates partial phase locking with the theta frequency. This result implies that

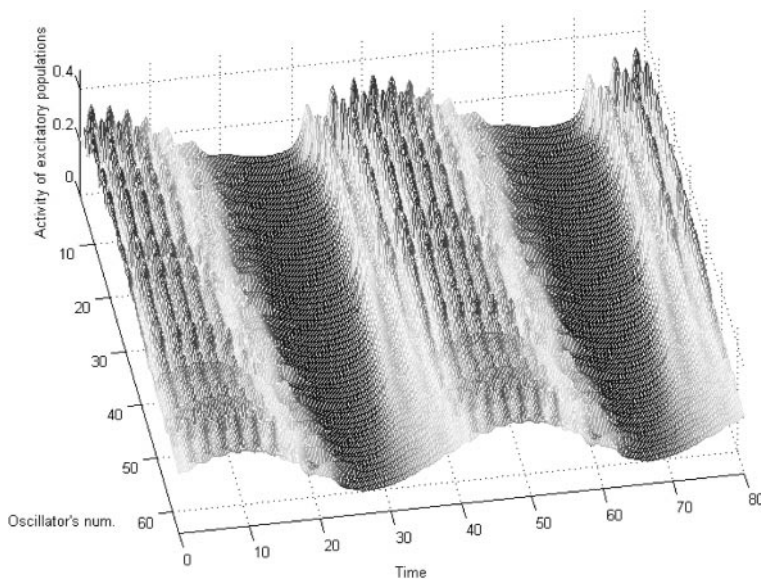


Fig. 12. Spatiotemporal activity patterns for the oscillatory mode of a single oscillator and random interoscillatory connections uniformly distributed between 0 and 0.1. $\beta_C = 0.3$, $\beta_S = 0.25$, $T = 40$, $\bar{P} = 1.5$, $Q = 0$, $N = 64$, $\phi_C = 0$, $\psi = 20$

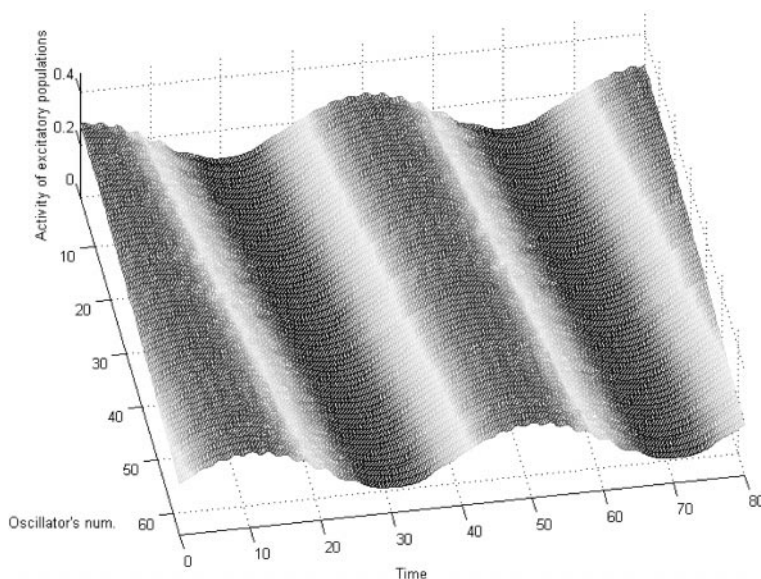


Fig. 13. Spatiotemporal pattern for lesion of the entorhinal cortex input. A single oscillator is in an oscillatory mode and connections between oscillators are random and uniformly distributed between 0 and 0.1. $\beta_C = 0$, $\beta_S = 0.25$, $T = 40$, $\bar{P} = 1.5$, $Q = 0$, $N = 64$, $\phi_C = 0$, $\psi = 20$

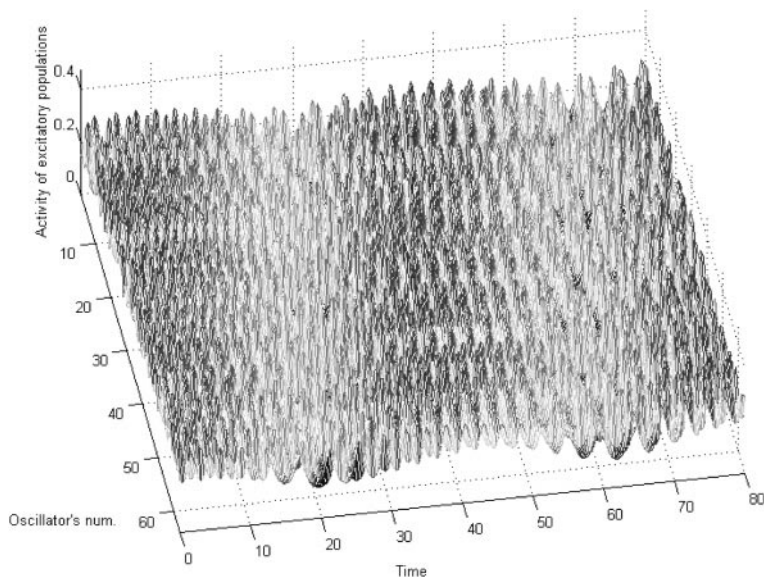


Fig. 14. Spatiotemporal pattern for lesion of the medial septum input. A single oscillator is in an oscillatory mode and connections between oscillators are random and uniformly distributed between 0 and 0.1. $\beta_C = 0.3$, $\beta_S = 0$, $T = 40$, $\bar{P} = 1.5$, $Q = 0$, $N = 64$, $\phi_C = 0$, $\psi = 20$

only proper phase deviations of inputs will provide synchronous activity of the hippocampus at the theta rhythm, and it shows that a spatial pattern of phase locking will result.

The amplitude model is used to describe the dynamics of a single hippocampal slice comprising excitatory (pyramidal neurons) and inhibitory (interneurons) neural populations. The response of the model is controlled by an input parameter acting on the excitatory population. Varying this parameter results in moving from the regime of stationary background activity to the regime of oscillatory activity through an Andronov-Hopf bifurcation. The hippocampal oscillator is forced by two oscillatory inputs, one acting on the excitatory population and the other on the inhibitory population. Our analysis demonstrates that the non-linear interaction of two oscillatory inputs can result in complex dynamics and spatiotemporal patterns.

We have studied this problem elsewhere from the point of view of spike trains using a three-dimensional array of integrate-and-fire units simulating both pyramidal cells and interneurons of the hippocampus. The results of these three-dimensional simulations are consistent with those described in this paper when suitably restricted.

As suggested by the VCON analysis, computer simulation of the neural oscillator model exhibits theta-rhythm phase-locking patterns for some combinations of septal and cortical afferent phase deviations. Our study of activity in the hippocampus is closely related to a theory developed by Miller (1991) concerning resonant, self-organizing phase-locked loops that might appear between the hippocampus and cortex. In his theory, the corticohippocampal interplay is considered to be a selection process for choosing appropriate resonant loops between the entorhinal cortex and the hippocampus, each with specific propagation times. These loops (specific paths) make possible complex information processing in the hippocampus. For example, memory and learning in the hippocampus depend on the theta-rhythm activity and phase relations between oscillations of laminar activity (Miller 1991).

Kryukov's theory (Kryukov et al. 1990) views the hippocampus as being a central executive that scans the cortical columns for resonant activity, and so forms a focus of attention. One might view Miller's and Kryukov's theories as being inconsistent with our results. However, these differences are reconciled when one views the feedback from the hippocampus as modulating or shaping the timing of the medial septum.

This paper shows that the timing of input signals can influence both the frequency and timing of outputs of spatial arrays of model neurons. We have shown (Borisjuk and Hoppensteadt 1998) that timing can also play an important role in modifying network connections during memorization of temporal sequences.

Acknowledgements. With great pleasure Roman Borisjuk would like to thank Prof. Frank Hoppensteadt and the Center for Systems Science at the Arizona State University for their hospitality during his stay there. R.B. is grateful to Prof. Olga Vinogradova for fruitful discussions about the hippocampus. R.B. research was supported in part by Grant 99-04-49112 from Russian Foundation of Fundamental Research. FH is supported in part by NSF Grant DMS 98-05514.

References

- Amaral D, Witter M (1989) The three-dimensional organization of the hippocampal formation: a review of anatomical data. *Neuroscience* 31:571–591
- Amaral DG, Witter MP (1995) Hippocampal formation. In: Paxinos G (ed) *The rat nervous system*, 2nd edn. Academic Press, New York, pp 443–494
- Berger T, Chauvet G, Scalabassi R (1994) A biologically based model of functional properties of the hippocampus. *Neural Networks* 7:1031–1064
- Bibbig A, Wennekers Th, Palm G (1995) A neural network model of the cortico-hippocampal interplay and the representation of contexts. *Behav Brain Res* 66:169–175
- Blum KI, Abbott LF (1995) A model of spatial map formation in the hippocampus of the rat. *Neural Comp* 8:85–93
- Borisjuk GN, Borisjuk RM, Kazanovich YB, Luzyanina TB, Turova TS, Cymbalyuk GS (1992) Oscillatory neural networks. *Mathematics and applications (in Russian)*. *Math Model* 4:3–43

- Borisyuk GN, Borisyuk RM, Khibnik AI, Roose D (1995) Dynamics and bifurcations of two coupled neural oscillators with different connection types. *Bull Math Biol* 57:809–840
- Borisyuk RM, Hoppensteadt FC (1998) Memorizing and recalling spatial-temporal patterns in an oscillator model of the hippocampus. *Biosystems* 48:3–10
- Borisyuk R, Kazanovich Ya (1995) Synchronization of neural oscillators: attention modeling. In: Herrmann HJ, Wolf DE, Poeppel E (eds) *Proceedings of Workshop Supercomputers in brain research: from tomography to neural networks, SCBR'94* Juelich, Germany, World Sci Publ Co, pp 407–413
- Borisyuk RM, Kirillov AB (1992) Bifurcation analysis of a neural network model. *Biol Cybern* 66:319–325
- Bragin A, Jando G, N'adasdy Z, Hetke J, Wise K, Buzsa'ki G (1995) Gamma (40–100 Hz) oscillation in the hippocampus of the behaving rat. *J Neurosci* 15:47–60
- Burgess N, Recce M, O'Keefe J (1994) A model of hippocampal function. *Networks* 7:1065–1082
- Buzsaki G, Bragin A, Chrobak JJ, N'adasdy Z, Sik A, Hsu M, Ylinen A (1994) Oscillatory intermittent synchrony in the hippocampus: relevance to memory trace formation. In: Buzsaki G, Llinas R, Singer W, Berthoz A, Christen Y (eds) *Temporal coding in the brain*. Springer, Berlin. 145–172
- Dutar P, Bassant M-H, Senut MC, Lamour Y (1995) The septo-hippocampal pathway: structure and function of a central cholinergic system. *Physiol Rev* 75:393–427
- Eichenbaum H (1997) How does the brain organize memories? *Science* 277:393–332
- Gray Ch (1994) Synchronous oscillations in neural systems: mechanisms and functions. *J Comput Neurosci* 1:11–38
- Hasselmo ME, Schnell E, Barkai E (1995) Learning and recall at excitatory recurrent synapses and cholinergic modulation in hippocampal region CA3. *J Neurosci* 15:5249–5262
- Hodgkin AL (1948) The local electric changes associated with repetitive action in a non-medulated axon. *J Physiol* 107:165–181
- Hoppensteadt FC (1997) *An introduction to the mathematics of neurons. Modeling in the frequency domain*, 2nd edn. (1st edition in 1986). Cambridge University Press, New York
- Hoppensteadt FC, Izhikevich EM (1997) *Weakly connected neural networks*. Springer, New York, Berlin, Heidelberg
- Iijima T, Witter M, Ishikawa M, Tominaga T, Kajiwara R, Matsumoto G (1996) Entorhinal-hippocampal interactions revealed by real-time imaging. *Science* 272:1176–1179
- Isaacson R (1982) *The limbic system*. Plenum Press, London
- Ishizuka N, Weber J, Amaral DG (1990) Organization of intra-hippocampal projections originating from CA3 pyramidal cells in the rat. *J Comp Neurol* 295:580–623
- Kazanovich YB, Borisyuk RM (1994) Synchronization in a neural network with a central element. *Biol Cybern* 71:177–185
- Kryukov VI, Borisyuk GN, Borisyuk RM, Kirillov AB, Kovalenko Yeu (1990) Metastable and unstable states in the brain. In: Dobrushin RL, Kryukov VI, Toom AL (eds) *Stochastic cellular systems: ergodicity memory morphogenesis*. Manchester University Press, Manchester, pp 225–358
- McNaughton BL, Barnes CA, Gerrard JL, Gothard K, Jung MW, Knierim JJ, Kudrimoti H, Qin Y, Skaggs WE, Suster M, Weaver KL (1996) Deciphering the hippocampal polyglot: the hippocampus as a path integration system. *J Exp Biol* 199:173–185
- McNaughton BL, Leonard B, Chen L (1989) Cortical-hippocampal interactions and cognitive mapping: a hypothesis based on re-integration of the parietal and inferotemporal pathways for visual processing. *Psychobiology* 17:230–235
- Miller R (1991) *Cortico-hippocampal interplay*. Springer, New York, Berlin, Heidelberg
- O'Keefe J, Nadel L (1978) *The hippocampus as a cognitive map*. Clarendon Press, Oxford
- O'Keefe J, Recce ML (1993) Phase relationship between hippocampal place units and the EEG theta rhythm. *Hippocampus* 3:317–330
- Palm G (1993) Cell assemblies, coherence and cortico-hippocampal interplay. *Hippocampus* 3:219–225
- Skaggs WE (1995) *Relations between the theta rhythm and activity patterns of hippocampal neurons*. PhD Diss, University Arizona, Tucson
- Sutherland RJ, Rudy JW (1989) Configural association theory: the role of the hippocampal formation in learning memory and amnesia. *Psychobiology* 17:129–144
- Traub R, Miles R (1991) *Neural networks of the hippocampus*. Cambridge University Press, New York
- Traub RD, Whittington MA, Colling SB, Buzsa'ki G, Jefferys JGR (1996) Analysis of gamma rhythm in the rat hippocampus in vitro and in vivo. *J Physiol* 493:471–484
- Traub R, Jefferys J, Whittington M (1997) Simulation of gamma rhythms in networks of interneurons and pyramidal cells. *J Comput Neurosci* 4:141–150
- Treves A, Rolls EI (1994) Computational analysis of the role of the hippocampus in memory. *Hippocampus* 4:374–391
- Tsodyks M, Sejnowski T (1995) Associative memory and hippocampal place cells. *Int J Neur Syst* 6:81–86
- Tsukada M, Aihara T, Saito H-A, Kato H (1996) Hippocampal LTP depends on spatial and temporal correlation of inputs. *Neural Networks* 9:1357–1365
- Ventriglia F (1998) Computational experiments support a competitive function in the CA3 region of the hippocampus. *Bul Math Biol* 60:373–407
- Vinogradova OS (1995) Expression, control and probable functional significance of the neuronal theta-rhythm. *Prog Neurobiol* 45:523–582
- Wang X-J, Buzsa'ki G (1996) Gamma oscillation by synaptic inhibition in a hippocampal interneuronal network model. *J Neurosci* 16:6402–6413
- Wilson HR, Cowan JD (1972) Excitatory and inhibitory interactions in localized populations of model neurons. *Biophys J* 12:1–24
- Wilson MA, McNaughton BL (1993) Dynamics of the hippocampal ensemble code for space. *Science* 261:1055–1058
- Zola-Morgan S, Squire LR, Amaral DG (1986) Human amnesia and the medial temporal region. Enduring memory impairment following a bilateral lesion limited to field CA1 of the hippocampus. *J Neurosci* 6:2950–2967